Proceedings of Science and Mathematics
Faculty of Science, Universiti Teknologi Malaysia
Volume 33, 2026, page 17-24

# Comparative Study of a Molecularly Imprinted Polymer-based Electrochemical Sensor for Free Fatty Acid Detection

**Horward Wong[a], Faizuan Abdullah[a], Amirah Kamaruddin[a]***
[a] Department of Chemistry, Faculty of Science, Universiti Teknologi Malaysia, Johor Bahru, Johor, Malaysia
*Corresponding author: amirahfarhan@utm.my

**Abstract**
Fossil fuel overuse drives the search for cleaner energy sources like biodiesel, but high free fatty acids (FFAs) in used cooking oil (UCO) hinder its production. Current FFA detection methods are costly and inefficient. This study aims to develop a fast, affordable electrochemical molecularly imprinted polymer (MIP) sensor using a screen-printed carbon electrode (SPCE) modified with functionalised multi-walled carbon nanotubes (FMWCNTs) and zinc oxide nanoparticles (ZnONPs), by varying the concentration of ZnONPs for the detection of FFAs, specifically oleic acid, in UCO. The sensor was fabricated by electropolymerising methacrylic acid monomer with oleic acid template onto SPCE-modified with FMWCNTs and ZnONPs. Characterisation techniques, including attenuated total reflectance-Fourier transform infrared spectroscopy (ATR-FTIR), atomic force microscopy, thermogravimetric analysis, and cyclic voltammetry, confirmed the successful fabrication and modification of the sensor, although FTIR analysis revealed some overlapping peaks and residual oleic acid, suggesting incomplete template removal. The sensor's performance was evaluated against the traditional titration method. The best-performing sensor, modified with 2.4 mg/mL ZnONPs ($R^2$ of 0.911), exhibited a detection limit (LOD) of 1.91 mM and a quantification limit (LOQ) of 5.79 mM. While the titration method demonstrated superior sensitivity and linearity ($R^2$ = 0.999) with very low LOD and LOQ with 0.2 mM and 0.6 mM, respectively, the MIP-based sensor showed promising potential for rapid, on-site FFA detection with further optimisation. The study highlights the application of MIPs in enhancing the selectivity and sensitivity of electrochemical sensors, contributing to the development of greener and more sustainable analytical methods for biodiesel production.
**Keywords:** cement; XRF; XRD; ICP-OES; compressive strength

## Introduction

The rising global energy demand and the environmental impacts of fossil fuel combustion have intensified the search for renewable alternatives. Biodiesel, particularly from non-edible sources, offers a promising route toward sustainability [1]. Used cooking oil (UCO) is widely recognised as an economical and environmentally friendly biodiesel feedstock due to its low cost and waste reduction benefits [2]. However, the presence of free fatty acids (FFAs) such as oleic acid can reduce biodiesel yield by promoting soap formation during the transesterification process [3, 4]. Accurate detection of FFAs is therefore essential to ensure efficient biodiesel production. To address the limitations of conventional detection methods, this study presents the development of a molecularly imprinted polymer (MIP)-based electrochemical sensor tailored for oleic acid detection. The sensor was fabricated by electropolymerising methacrylic acid (MAA) monomer on a screen-printed carbon electrode (SPCE) modified with functionalised multi-walled carbon nanotubes (FMWCNTs) and varying concentrations of

zinc oxide nanoparticles (ZnONPs) [5]. Sensor performance was characterised by using several techniques and compared against the traditional titration method to evaluate sensitivity and reliability.

Accurate determination of FFAs in UCO is critical for biodiesel quality control. Among traditional approaches, acid-base titration is the most commonly used method due to its simplicity. However, it is prone to inaccuracy due to reliance on visual endpoints and interference from impurities in oil matrices, which can lead to misinterpretation of the endpoint and inconsistent titration results. Additionally, this method requires large amounts of solvents and reagents, which raises safety and environmental concerns. Advanced analytical methods such as gas chromatography (GC) and high-performance liquid chromatography (HPLC) offer better accuracy and reproducibility, yet are time-consuming, expensive, and require trained personnel [6, 7]. These drawbacks highlight the need for alternative FFA detection techniques that are rapid, low-cost, and suitable for real-time, on-site applications.

Electrochemical sensors are gaining popularity in FFA detection due to their high sensitivity, fast response time, and low sample volume requirement [8]. A promising enhancement involves integrating MIPs, which act as synthetic receptors with high affinity and selectivity for specific target molecules like oleic acid [9]. MIPs are chemically stable and can withstand variations in pH and temperature, making them suitable for use in complex matrices. The fabrication of MIPs through electropolymerisation on SPCEs enables the production of robust, low-cost sensors for field analysis [5]. Further performance enhancements have been achieved by incorporating nanomaterials such as ZnONPs and FMWCNTs. ZnONPs offer high electrical conductivity and a large surface-to-volume ratio, while FMWCNTs increase electron mobility and provide a favourable interface for molecular interactions [10, 11].

**Materials and methods**

The methodology in this study involved several stages: the development of five different SPCE/FMWCNTs/ZnONPs/MIPs by varying ZnONPs concentrations, the characterisation of the modified sensors using various techniques, and the comparison of performance between the sensor and the titration method.

The SPCE underwent activation and cleaning at room temperature using CV on a DropSens system. The nanostructured carbon working electrode of the SPCE was immersed in a 0.1 M $H_2SO_4$ solution and subjected to a potential range of -1.4 V to 1.4 V for 15 cycles at a scan rate of 0.1 V/s. After cleaning, the SPCE was rinsed with deionised water and thoroughly dried before modification [12].

The SPCE fabrication process involved using the drop-coating method to apply 1.2 mg/mL of FMWCNTs and varying concentrations of ZnONPs (0.6 – 3.0 mg/mL) onto the electrode surface. The suspensions were sonicated for 30 minutes to achieve stability before drop-casting. Both suspensions were then drop-cast onto the active area of the SPCE, forming the SPCE/FMWCNTs/ZnONPs structure [13].

The next step involved the in-situ electropolymerisation of the MIP onto the SPCE surface. MAA served as the functional monomer, while oleic acid, EGDMA, and AIBN were used as the template molecule, crosslinker, and initiator, respectively. 100 µL of the prepared 0.5 mM MAA, 100 µL of 0.1 mM oleic acid, 100 µL of 0.05 M EDGMA and 100 µL of 0.1 mM AIBN were mixed. These mixtures were then drop-coated onto modified SPCEs. Subsequently, the MIPs were electropolymerised using CV with 5mM $K_3[Fe(CN)_6]$ in 0.1 M KCl method with a potential range of -1.4 V to 1.4 V for 15 cycles at a scan rate of 0.1 V/s [5]. A 5% acetic acid solution was prepared and stirred continuously using a magnetic stirrer. An electrode was then introduced into the mixture for 15 seconds to remove the target analyte, forming cavities in the MIP for subsequent binding.

The modified SPCE was characterised physically and electrochemically using ATR-FTIR, AFM, TGA, and CV. ATR-FTIR analysis provided information on the functional groups present in the sensor. AFM was used to examine the electrode's surface morphology features at high resolution, offering insights into the surface roughness and distribution of the nanomaterials. TGA analysis was conducted to evaluate the thermal stability and decomposition profile of the modified SPCE. These characterisation techniques provided valuable information on the structural modifications achieved through the coating

process with FMWCNT, ZnONPs and MIPs. Furthermore, CV was employed to assess the electrochemical performance of the modified SPCE [14].

Standard solutions of oleic acid at concentrations of 0.5 mM, 1.0 mM, 1.5 mM, 2.0 mM, and 2.5 mM were prepared using isopropanol as the solvent. Approximately 0.5 mL of phenolphthalein indicator was added to each flask. The solutions were then titrated with 0.1 N KOH until a pale pink colouration persisted, indicating the endpoint. The volume of KOH used for each titration was recorded accordingly [15].

Standard solutions of oleic acid (0.5 mM, 1.0 mM, 1.5 mM, 2.0 mM, and 2.5 mM) were prepared, and CV measurements were conducted for each sensor. After obtaining the results from both the electrochemical sensor and the titration method, calibration plots were generated for each method, and their LOD, LOQ, and $R^2$ were calculated based on these plots.

**Results and discussion**

**Figure 1** confirms the successful modification of the SPCE/FMWCNTs/ZnONPs sensor using FTIR analysis.

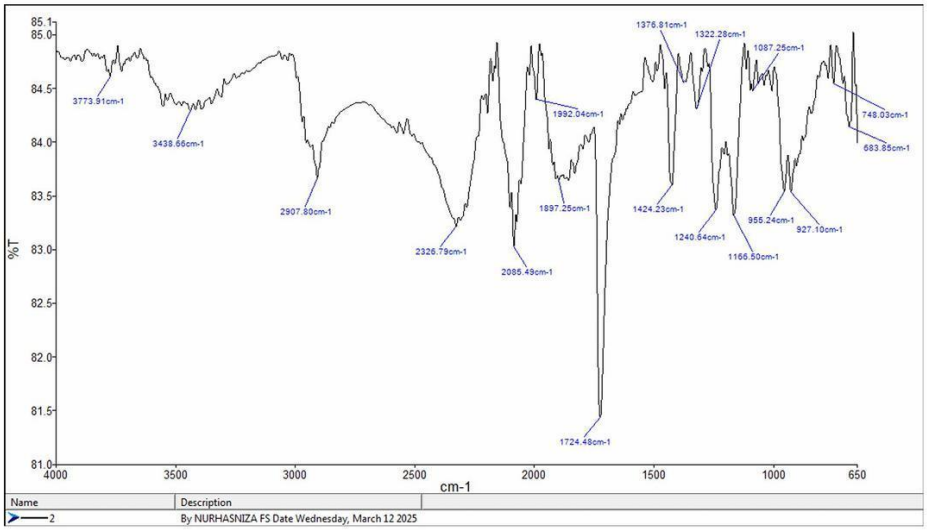


**Figure 1** FTIR analysis of SPCE/FMWCNTs/ZnONPs.

The broad peak at 3438.65 $cm^{-1}$ corresponded to O–H stretching from hydroxyl groups on functionalized FMWCNTs and Zn–OH due to moisture absorption [16]. A peak at 2907.80 $cm^{-1}$ indicated C–H defects from carboxyl group incorporation [17]. The 1424.23 $cm^{-1}$ peak was assigned to C=C stretching in graphitic CNTs, while peaks from 1070–1330 $cm^{-1}$ indicated C–O stretching. The 748.03 $cm^{-1}$ peak represented Zn–OH bending, and the 927.10 $cm^{-1}$ peak confirmed Zn tetrahedral coordination [13]. These results verified the successful incorporation of FMWCNTs and ZnONPs, enhancing the sensor's electrochemical properties.

**Figure 2** shows changes in functional groups before and after removing oleic acid from the MMA-based MIP. The broad O–H stretching peak at 3200–3500 $cm^{-1}$ indicated hydroxyl groups from oleic acid, and its persistence after removal suggested incomplete template extraction. The C=O stretching peaks at 1723.44 $cm^{-1}$ and 1721.54 $cm^{-1}$ confirmed carbonyl groups from both MMA and oleic acid. A C=C stretching peak near 1650 $cm^{-1}$ pointed to residual unpolymerized MMA and oleic acid. The C–H stretching vibration became clearer at 2905.20 $cm^{-1}$ after removal, showing the presence of alkyl groups. C–O stretching peaks appeared at 1233.15 $cm^{-1}$ and 1244.80 $cm^{-1}$ before and after removal, respectively.

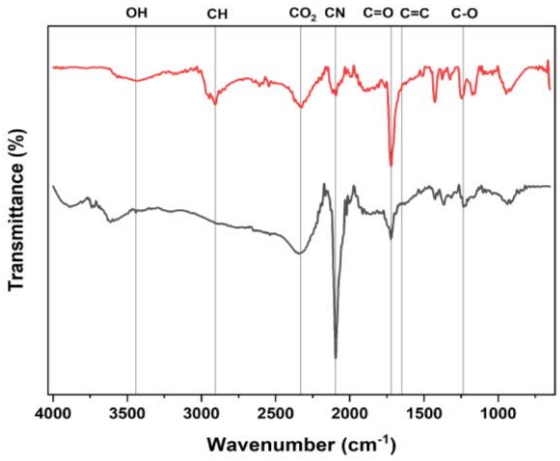


**Figure 2** Comparison of FTIR Analysis of SPCE/FMWCNTs/ZnONPs/MIPs before and after template removal. Red line indicates modified SPCE (after removal of template); Black line indicates modified SPCE (before removal of template).

AFM analysis was used to examine the surface topography of imprinted and non-imprinted polymers. Using tapping mode over a 350 × 350 nm area, 3D images and measurements of average and RMS roughness were obtained. As shown in **Table 1**, the average roughness increased from 52.93 nm (MIP with template) to 95.61 nm (empty MIP), with a similar trend in RMS roughness. This increase indicates the formation of imprinted cavities after template (oleic acid) removal, enhancing the surface texture and enabling template re-adsorption [18, 19].

**Table 1:** AFM results of different modified conditions of SPCE.

| Condition of SPCE | 3D Surface Topography | Average Roughness, Ra (nm) | Root mean square roughness, Rq (nm) |
|---|---|---|---|
| Bare SPCE | 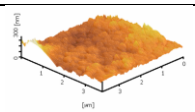 | 31.95 | 41.18 |
| SPCE/FMWCNTs | 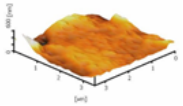 | 40.54 | 58.25 |
| SPCE/FMWCNTs/ZnONPs | 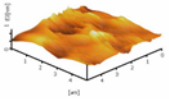 | 87.08 | 112.60 |
| SPCE/FMWCNTs/ZnONPs/MIPs (Before removal of template) | 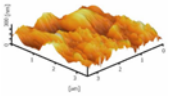 | 52.93 | 64.95 |
| SPCE/FMWCNTs/ZnONPs/MIPs (After removal of template) | 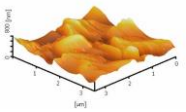 | 95.61 | 122.00 |

Based on TGA analysis, **Figure 3** shows that the SPCE/FMWCNTs/ZnONPs/MIPs sensor had good thermal stability, with only 0.68% weight loss. No significant degradation was observed in the 280–450 °C range, typically associated with polymer breakdown [20], likely due to the low MAA content in the 5 µL MIP solution. Similarly, minimal weight change in the 450–500 °C range was attributed to the small amount (1 mM) of oleic acid used.

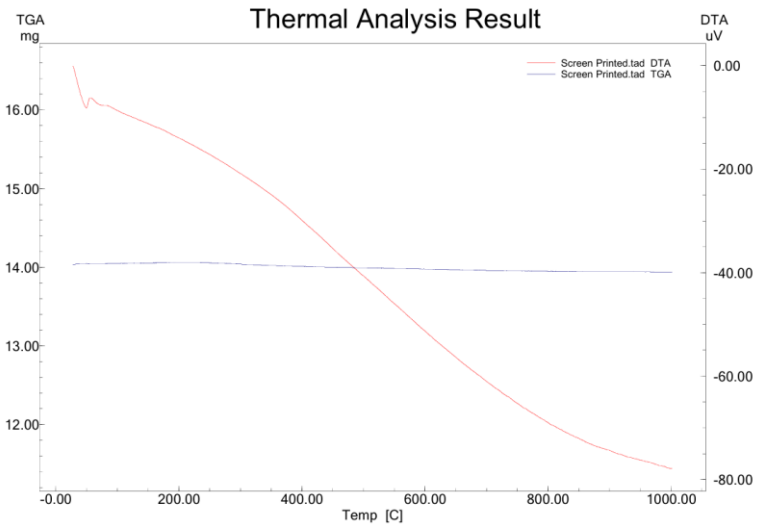


**Figure 3** TGA curve for SPCE/FMWCNTs/ZnONPs/MIPs. Red line indicates result of DTA; Black line indicates the result of TGA.

The electrochemical performance of the fabricated sensor was evaluated using cyclic voltammetry (CV) in a 5 mM $[Fe(CN)_6]^{3-}$ solution with 0.1 M KCl as the supporting electrolyte. Scans were performed from –1.4 V to 1.4 V at 0.1 V/s for 15 cycles. All modified SPCEs showed clear redox peaks for the $[Fe(CN)_6]^{3-/4-}$ couple. The bare SPCE displayed weak peak currents, indicating poor electrochemical activity [16].

Modification with ZnONPs and FMWCNTs significantly enhanced the anodic and cathodic peak currents, attributed to increased surface area and improved electron transfer [21, 22]. However, unexpectedly, both the empty MIP and MIP with template showed higher peak currents than SPCE/FMWCNTs/ZnONPs, contrary to typical behaviour where MIPs reduce current by limiting probe access.

Theoretically, MIPs should lower the response by filling spaces between nanotubes and blocking redox probe access, especially in the MIP with template [18]. The higher-than-expected currents may be due to uneven MIP coating from manual drop-casting, resulting in incomplete surface coverage. This could leave parts of the electrode exposed, allowing direct electron transfer and increased current, mimicking the response of a more conductive, non-imprinted surface.

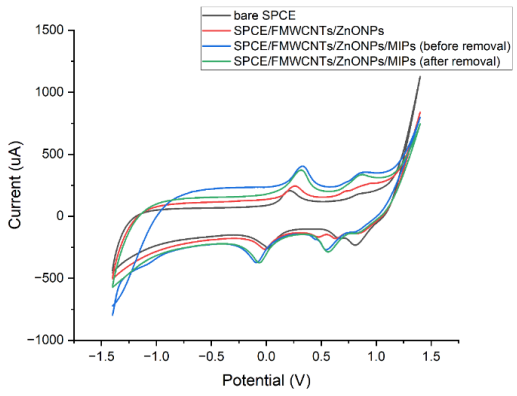


**Figure 4** The CV characterisation of (a) bare SPCE, (b) SPCE/FMWCNTs/ZnONPs, (c) SPCE/ FMWCNTs/ZnONPs/MIPs (before removal of template), (d) SPCE/ FMWCNTs/ZnONPs/MIPs (after removal of template).

During CV analysis for oleic acid quantification, anodic and cathodic peaks were observed in each cycle. However, since oleic acid is non-electroactive, these peaks (around +0.3 V and –0.1 V) likely correspond to the redox activity of $[Fe(CN)_6]^{3-/4-}$ in the electrolyte. Despite its non-electroactive nature, oleic acid can still influence electrochemical responses by interacting with the sensor surface, thereby enhancing electron transfer and increasing peak currents. Electrochemical Impedance Spectroscopy further supports this, as increased oleic acid concentrations were linked to decreased charge transfer resistance, indicating improved conductivity. Thus, oleic acid indirectly enhances the redox response of $[Fe(CN)_6]^{3-/4-}$, making CV peak currents a viable proxy for its quantification.

**Figure 5** shows the CV response of SPCE/FMWCNTs/ZnONPs/MIPs to increasing oleic acid concentrations (0.0–2.5 mM), with distinct anodic (0.3 V) and cathodic (–0.1 V) peaks. Peak currents increased with concentration, indicating that oleic acid enhances electron transfer via interactions with the sensor surface or MIP layer.

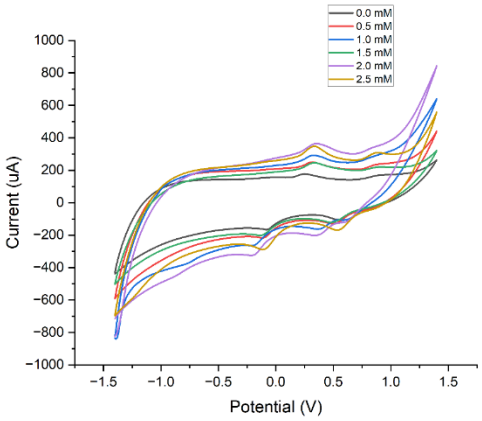


**Figure 5** CV analysis of modified SPCE with 0.6 mg/mL ZnONPs performed at varying oleic acid concentrations.

Calibration plots were generated for SPCEs modified with different ZnONPs concentrations, and analytical parameters (LOD, LOQ, $R^2$) are summarised in **Table 2**. The SPCE with 2.4 mg/mL ZnONPs performed best, showing the lowest LOD/LOQ, making it suitable for detecting oleic acid in UCO, which typically contains ~15.46 M oleic acid in a 1 g/10 mL sample [23].

**Table 2:** The LOD, LOQ, $R^2$ and calibration plot equations of all modified SPCE with different concentrations of ZnONPs.

| Concentration of ZnONPs (mg/mL) | LOD (mM) | LOQ (mM) | $R^2$ |
|---|---|---|---|
| 0.6 | 3.32 | 10.05 | 0.772831 |
| 1.2 | 3.69 | 11.19 | 0.733052 |
| 1.8 | 2.75 | 8.34 | 0.831663 |
| 2.4 | 1.91 | 5.79 | 0.911156 |
| 3.0 | 60.56 | 140.07 | 0.010103 |

This sensor also achieved the highest $R^2$ (0.911), though still below the ideal threshold of >0.98 [24], suggesting room for optimisation. The superior performance at 2.4 mg/mL ZnONPs is likely due to optimal surface morphology and enhanced electron transfer [25]. Thus, there is a high probability that the modified sensor will function effectively under this condition. In contrast, 3.0 mg/mL ZnONPs resulted in poor performance (LOD: 60.56 mM, LOQ: 140.07 mM, $R^2$: 0.01), likely due to nanoparticle aggregation and structural defects that hinder charge transport [26].

The SPCE modified with 2.4 mg/mL ZnONPs, which showed the best analytical performance, was compared with the conventional acid-base titration method (**Table 3**). While titration achieved

superior sensitivity (lower LOD/LOQ) and excellent linearity ($R^2 = 0.999$), the sensor showed slightly lower performance ($R^2 = 0.911$), indicating a need for further optimisation.

Despite this, the sensor offers key advantages: portability, rapid on-site testing, and reduced human error compared to manual titration, as noted by previous researchers [27]. Due to these advantages, it has strong potential as a practical alternative for FFA quantification, even though it showed poorer results than the titration method in terms of accuracy and precision.

**Table 3:** The comparison of LOD, LOQ, $R^2$ between modified SPCE and titration method.

| Analytical Parameter | Modified SPCE | Titration |
|---|---|---|
| LOD | 1.910524 | 0.19721368 |
| LOQ | 5.789466 | 0.5976172 |
| $R^2$ | 0.911156 | 0.999 |

## Conclusion

This research successfully developed and evaluated five electrochemical sensors incorporating MIPs for oleic acid detection, confirmed by ATR-FTIR, AFM, TGA, and CV analyses. SPCEs were modified by drop-casting a fixed amount of FMWCNTs with varying ZnONP concentrations. Standard oleic acid solutions (0.5–2.5 mM) were tested using CV to obtain redox peak currents, and calibration plots were used to determine LOD, LOQ, and $R^2$ values. Among the sensors, the one with 2.4 mg/mL ZnONPs showed the best performance ($R^2 = 0.911$), although still lower than the titration method ($R^2 = 0.999$). Overall, the study achieved its goals of fabricating, characterizing, and evaluating the sensors, and comparing them to titration. Future work should focus on real sample testing and further optimisation for improved sensitivity and selectivity.

## Acknowledgement

The authors would like to thank the Faculty of Science, Universiti Teknologi Malaysia for the facilities provided to accomplish complete tests.

## References

1. Bajwa, W.*, et al.*, *Optimization of biodiesel yield from waste cooking oil and sesame oil using RSM and ANN techniques.* Heliyon, 2024. **10**(15): p. e34804.
2. Orjuela, A. and J. Clark, *Green chemicals from used cooking oils: Trends, challenges, and opportunities.* Current Opinion in Green and Sustainable Chemistry, 2020. **26**: p. 100369.
3. Roslan, N.*, et al.*, *Esterification Reaction of Free Fatty Acid in Used Cooking Oil using Sulfonated Hypercrosslinked Exchange Resin as Catalyst.* Chemical Engineering Research and Design, 2021. **180**.
4. Wan Osman, W.N.A.*, et al.*, *Comparative review of biodiesel production and purification.* Carbon Capture Science & Technology, 2024. **13**: p. 100264.
5. Masekela, D. and L. Dlamini, *Molecularly Imprinted and MXene-based Electrochemical Sensors for Detecting Pharmaceuticals and Toxic Compounds: A concise review.* Journal of Environmental Chemical Engineering, 2024. **12**: p. 114569.
6. Almeida-Trapp, M.*, et al.*, *Development, validation, and application of an HPLC-MS/MS method for quantification of oxidized fatty acids in plants.* J Chromatogr B Analyt Technol Biomed Life Sci, 2021. **1186**: p. 123006.
7. Jayaprabakar, J.*, et al.*, *Development of Free Fatty Acid (FFA) monitoring device for evaluation of oil samples used for biodiesel production.* Heliyon, 2024. **10**(17): p. e37118.
8. Ezzah, F.*, et al.*, *Evolution of MXene and its 2D heterostructure in electrochemical sensor applications.* Coordination Chemistry Reviews, 2022. **471**: p. 214755.
9. Ostovan, A.*, et al.*, *Greenificated Molecularly Imprinted Materials for Advanced Applications.* Advanced Materials, 2022. **34**(42): p. 2203154.

10. Faradilla, P.*, et al.*, *Electrochemical sensor based on screen printed carbon electrode–zinc oxide nano particles/molecularly imprinted-polymer (SPCE–ZnONPs/MIP) for detection of sodium dodecyl sulfate (SDS).* RSC Advances, 2022. **12**(2): p. 743-752.
11. Baek, I.-G.*, et al.*, *Enhancing the electrochemical performance of free-standing electrodes using multi-walled carbon nanotubes functionalized with PVP/SDBS mixed dispersant.* Journal of Energy Storage, 2024. **103**: p. 114362.
12. Hosseinzadeh, B.*, et al.*, *Detection of the antipsychotic drug cariprazine using a low-cost MIP-based electrochemical sensor and its electrooxidation behaviour.* Microchemical Journal, 2024. **207**: p. 112105.
13. Adesanya, F. and O. Fayemi, *Anthracene electrochemical sensor at fMWCNTs/ZnO modified glassy carbon electrode.* International Journal of Electrochemical Science, 2023. **18**: p. 100382.
14. Brahma, B.*, et al.*, *Interference-free electrocatalysis of p-chloro meta xylenol (PCMX) on uniquely designed optimized polymeric nanohybrid of P(EDOT-co-OPD) and fMWCNT modified glassy carbon electrode.* Analytica Chimica Acta, 2021. **1168**: p. 338595.
15. Samuel, S.*, et al.*, *Novel Eco-Friendly Acid-base Indicators from Innovative Plant-Based sources: Water-based extraction and Applications in Titration.* Next Research, 2024. **2**: p. 100129.
16. Balram, D.*, et al.*, *Surface functionalization of CNTs with amine group and decoration of begonia-like ZnO for detection of antipyretic drug acetaminophen.* Applied Surface Science, 2021. **559**: p. 149981.
17. Vardhaman, B.S.A., M. Amarnath, and J. Ramkumar, *Experimental investigations to enhance the tribological behaviour of biodegradable oil by using manganese doped ZnO/FMWCNTs nanomaterials as lubricant additive.* Diamond and Related Materials, 2022.
18. Roushani, M., S. Rahimitodehrodi, and Z. Mirzaei Karazan, *An electrochemical sensor based on molecularly imprinted copolymer for the detection of Osimertinib.* Materials Science and Engineering: B, 2025. **313**: p. 117891.
19. Singh, R. and M. Singh, *Highly selective and specific monitoring of pollutants using dual template imprinted MIP sensor.* Journal of Electroanalytical Chemistry, 2022. **926**: p. 116939.
20. Do Prado Ferreira, M.*, et al.*, *Development of method for SARS-CoV-2 spike protein determination in saliva samples at fg mL−1 levels using electrochemically controlled preconcentration and molecularly imprinted polypyrrole sensor.* Microchemical Journal, 2024.
21. Ismail, S.*, et al.*, *Electrochemical Detection of Arsenite Using a Silica Nanoparticles-Modified Screen-Printed Carbon Electrode.* Materials, 2020. **13**(14): p. 3168.
22. Jalalvand, A.R., *Fabrication of a novel molecularly imprinted biosensor assisted by multi-way calibration for simultaneous determination of cholesterol and cholestanol in serum samples.* Chemometrics and Intelligent Laboratory Systems, 2022. **226**: p. 104587.
23. Suzihaque, M.U.H.*, et al.*, *Biodiesel production from waste cooking oil: A brief review.* Materials Today: Proceedings, 2022. **63**.
24. Sousa, M.*, et al.*, *DEVICE FOR CALIBRATING ELECTROCHEMICAL DISSOLVED OXYGEN SENSORS.* Química Nova, 2025.
25. Patil, V.B.*, et al.*, *Nanostructured ZnO-Based Electrochemical Sensor with Anionic Surfactant for the Electroanalysis of Trimethoprim.* Bioengineering, 2022. **9**(10): p. 521.
26. Sledevskis, E.*, et al.*, *Impact of ZnO Nanostructure Morphology on Electrochemical Sensing Performance for Lead Ion Detection in Real Water Samples.* Chemosensors, 2025. **13**(2): p. 62.
27. Smart, A.*, et al.*, *Screen-printed carbon based biosensors and their applications in agri-food safety.* TrAC Trends in Analytical Chemistry, 2020. **127**: p. 115898.